RSC Advances

RSC Publishing

PAPER

View Article Online
View Journal | View Issue

Cite this: *RSC Adv.*, 2013, **3**, 20855

Enhanced doxorubicin transport to multidrug resistant breast cancer cells *via* TiO_2 nanocarriers†

Wenzhi Ren,[a] Leyong Zeng,[a] Zheyu Shen,[a] Lingchao Xiang,[a] An Gong,[a] Jichao Zhang,[b] Chengwen Mao,[b] Aiguo Li,[b] Tatjana Paunesku,[c] Gayle E. Woloschak,[c] Narayan S. Hosmane[d] and Aiguo Wu‡*[a]

Received 9th June 2013
Accepted 21st August 2013

DOI: 10.1039/c3ra42863j

www.rsc.org/advances

In order to overcome the multidrug resistance of breast cancer cells, doxorubicin was loaded onto TiO_2 nanoparticles in which the electrostatic interactions hold the drug and the nanoparticles together. The anticancer activity of this nanocomposite was evaluated in multidrug resistant breast cancer cells. In nanocomposite treated MCF-7/ADM cells, drug accumulation increased with enhanced anticancer activity about 2.4 times compared to that of doxorubicin alone. The potential mechanism of enhanced drug accumulation is ascribed to the fact that the nanocomposite directly transports the drugs into cells *via* internalization, bypassing the P-glycoprotein mediated doxorubicin pumping system. Our results reinforce that the nanocomposite, as a pH controlled drug release system, could be used to overcome multidrug resistance of human breast cancer cells.

1. Introduction

Chemotherapy is a major clinical approach for treatment of malignant tumors, but multidrug resistance of cancer cells is a major cause of failure in chemotherapy.[1] Over expression of P-glycoprotein (P-gp) on the membrane of cancer cells is considered to be the main mechanism of multidrug resistance.[2] It has been shown that P-gp can pump the drugs out, thus reducing intracellular drugs accumulation and weakening the anticancer effect of drugs.[3] The development of nanotechnology-driven drug delivery has the potential to revolutionize cancer therapy.[4,5] It has also been suggested that nanoparticle-based drug delivery may be able to circumvent P-glycoprotein mediated drug resistance in cancer and, consequently, reversing multidrug resistance.[6] Recently, a variety of inorganic nanocarriers, such as iron oxide nanoparticles, mesoporous silica nanoparticles, graphene oxide and titanium dioxide nanoparticles have been studied for drug delivery and therapy in multidrug resistant cancers.[7–12]

TiO_2 nanoparticle is a potential dynamic therapy agent in cancer therapy due to excellent biocompatibility and its unique photocatalytic properties.[13,14] Recently, our group has synthesized multifunctional Fe_3O_4–TiO_2 nanocomposite for potential applications in both magnetic resonance imaging (Fe_3O_4 constituent) and inorganic photodynamic therapy (TiO_2 constituent).[15] In addition, TiO_2 nanoparticles have also received much attention in the field of drug delivery of chemotherapeutic agents. Yan Chen *et al.* constructed DOX–TiO_2 composite as a drug delivery system.[16] The results show that this drug delivery system markedly increased the anticancer efficiency of the drug per dose in human SMMC-7721 hepatocarcinoma cells. In another study reported by Ying Qin *et al.*, TiO_2-loaded DOX was prepared by non-covalent complexation (TiO_2/DOX) and/or covalent conjugation (TiO_2–DOX). The therapeutic efficacy of two different loading modes was evaluated in C6 glioma cells. The results show that non-covalent TiO_2/DOX composite exhibited an increased cytotoxicity toward C6 cells compared to that of DOX alone, while the covalent composite of TiO_2/DOX showed decreased cytotoxicity.[17] The study indicates that the therapeutic efficacy is strongly dependent on its nature of interaction between TiO_2 nanoparticle surface and loaded DOX, which provides important information for the future applications of TiO_2 nanoparticles as drug carriers.

In our recent work, the Fe_3O_4@TiO_2 core–shell nanocomposites with 6–8 nm diameter have been explored as carriers for DOX delivery in drug-resistant ovarian carcinoma cells.[12] Accordingly, the DOX was loaded on TiO_2 surface by a labile

[a]*Key Laboratory of Magnetic Materials and Devices & Division of Functional Materials and Nanodevices, Ningbo Institute of Materials Technology and Engineering, Chinese Academy of Sciences, Ningbo, 315201, China*

[b]*Shanghai Synchrotron Radiation Facility, Shanghai Institute of Applied Physics, Chinese Academy of Sciences, Shanghai, 201204, China*

[c]*Department of Radiation Oncology, Northwestern University Feinberg School of Medicine Chicago, Illinois, 60611, USA*

[d]*Department of Chemistry & Biochemistry, Northern Illinois University DeKalb, Illinois, 60115-2862, USA*

† Electronic supplementary information (ESI) available. See DOI: 10.1039/c3ra42863j

‡ Present address: Room A510, No. 519 Zhuangshi Road, Ningbo City, Zhejiang Province, 315201, China, E-mail address: aiguo@nimte.ac.cn, Fax: +86 574 86685163, Tel: +86 574 86685039.

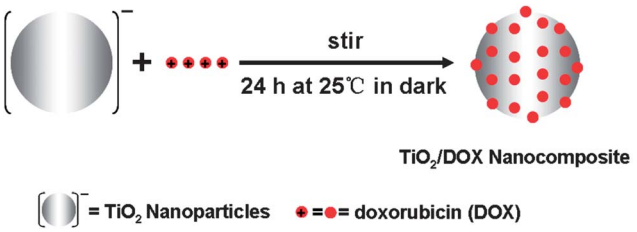

Scheme 1 Preparation of TiO_2/DOX nanocomposite. Molar ratio of DOX to TiO_2 was 0.55%. Surface of TiO_2 was modified by DOX through electrostatic interaction.

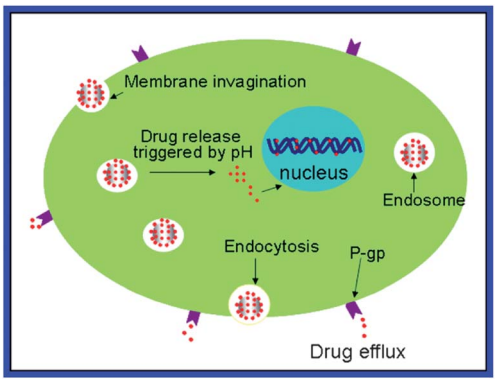

Scheme 2 Illustration of TiO_2/DOX overcoming multidrug resistance of MCF-7/ADM cells. The TiO_2/DOX nanocomposite transports the drug into intracellular cytoplasm *via* internalization. The drugs are released due to acidic environment of endosomes, and then accumulate in the nucleus, thus bypassing the P-gp mediated free DOX efflux.

7(non-covalent) bond, and this bond was sensitive at very low pH value, such as pH = 2. The results indicated that Fe_3O_4@-TiO_2 nanocarriers could enhance DOX uptake *via* clathrin-mediated endocytosis in multidrug resistant cancer cells. However, the Fe_3O_4@TiO_2 core–shell with DOX nanocomposites can not be broken upon acidification in the endosomes, for example, at pH = 4–5. It means that even if the drug, DOX can be accumulated inside the cancer cells, but it could not be effective on overcoming the multidrug resistance because the drugs are not easily released in the endosomes around pH = 4–5.[12] Thus, it is this challenge that led us to explore a weak acidic environment triggered drug release system to overcome drug-resistance, in which TiO_2 nanoparticles were used as carriers of DOX to forming TiO_2/DOX nanocomposites as shown in Scheme 1. We report herein the results of this study to confirm enhanced DOX transporting to human breast cancer (MCF-7/ADM) cells, thus overcoming the challenge of multidrug resistance. The results imply that TiO_2/DOX nanocomposite carriers transport DOX to the cytoplasm *via* internalization into endosomes bypassing the P-gp mediated DOX efflux. Presumably, the drugs are released in acidic endosomes, and then accumulated in intracellular nucleus (Scheme 2). Subsequently, TiO_2/DOX carriers reverse the multidrug resistance of MCF-7/ADM cells leading to enhanced anticancer activity of DOX up to 2.4 times when compared to that of DOX alone.

2. Experimental section

2.1. Materials

DOX, 3-(4,5-dimethylthiazol-2-yl)-2,5-diphenyltetrazolium bromide (MTT) and nuclear dyes Hoechst 33342 were obtained from Ningbo Hangjing biotechnology Co. Ltd. (Ningbo, China). The FITC labeled phalloidine was purchased from Sigma-Aldrich (Shanghai, China). Fetal bovine serum (FBS), Dulbecco's modified eagle's medium (DMEM), penicillin–streptomycin solution and trypsin–EDTA solution were purchased from Gibco (Grand Island, USA). All other reagents were of analytical grade.

2.2. Preparation and characterization of TiO_2/DOX nanocomposite

Colloidal TiO_2 nanoparticles were prepared by a method based on our previous work with modification.[18] Briefly, the nanoparticles were synthesized by drop-wise addition of $TiCl_4$ to cool ultrapure water, and were dialyzed with ultrapure water. Then, to improve the crystallinity of nanoparticles, the colloid was heated in a vessel at 200 °C for 10 hours, and the prepared colloidal TiO_2 was stored at 4 °C. Concentration of Ti was determined by ICP-MS (NexION 300, Perkin-Elmer, US), and was then diluted to 75 mM by ultrapure water. Colloidal TiO_2 nanoparticles (75 mM) were stirred, DOX (0.5 mM) was drop-wise added into the colloidal solution and stirred for 24 h. To ensure the stability of TiO_2/DOX, molar ratio of DOX to TiO_2 was adjusted to 0.0055. After stirring, the solution was centrifuged at 12 000 rpm for 30 minutes to separate TiO_2/DOX and the resulting nanocomposite was washed three times with ultrapure water and then stored at 4 °C. The UV-visible and infrared spectrum (IR) spectra of TiO_2, TiO_2/DOX and DOX were characterized respectively by NanoVue (GE healthcare, UK) and Fourier transform infrared spectrometer (Thermo Nicolet 6700, US). The zeta potentials and average diameters of TiO_2 nanoparticles and TiO_2/DOX nanocomposite were determined by Particle Size-Zeta Potential Analyzer (Nano ZS, Malvern Instruments Ltd, England). For measurement of TiO_2/DOX stability, 10 mL of TiO_2/DOX (7.5 mM/0.04 mM) colloidal solution was stored in ultrapure water for 7 days at room temperature, and the diameter of TiO_2/DOX was determined every day by the Particle Size-Zeta Potential Analyzer.

2.3. Drug release

DOX release experiments from TiO_2/DOX nanocomposites were investigated at pH = 7.4, pH = 5.0 and pH = 3.0. TiO_2/DOX (30 mM/0.165 mM) was transferred into three dialysis bags, and each bag contained 5 mL TiO_2/DOX. The dialysis bags were then immersed into 20 mL buffer solution at pH 7.4, 5.0, or 3.0 respectively. The dialysis solution was stirred for 48 hours at 37 °C. A 1 mL external dialysis solution was collected at scheduled time intervals, and replaced with the same fresh buffer solution. UV-visible absorptions of DOX concentration gradients from 0.25 to 0.0036 mM were characterized respectively by NanoVue. Concentration–absorption curve of DOX was calculated according to UV-visible absorptions of DOX concentration gradients. The amount of released DOX in the dialysis solution was then determined by UV-visible spectra.

2.4. Cell culture

Drug sensitive (MCF-7) and multidrug resistant (MCF-7/ADM) cell lines of human breast cancer were obtained from Ningbo No.2 Hospital. The cells were cultured in DMEM medium supplemented with 10% fetal bovine serum, 100 U mL^{-1} penicillin, and 100 μg mL^{-1} streptomycin, and in a humidified incubator at 37 °C in air with 5% CO_2.

2.5. *In vitro* cytotoxicity of TiO_2 nanoparticles

Cytotoxicity of TiO_2 nanoparticles in MCF-7 and MCF-7/ADM cells was measured by the MTT assay. Cells were grown in 96-well plates with a number of 1×10^4 cells per well for 24 h and the cells were then incubated with fresh DMEM or various concentrations of TiO_2 nanoparticles containing DMEM for another 24 h. After 24 h incubation, 10 μL MTT (5 mg mL^{-1} in PBS) was added into each well. After 4 h of treatment, the MTT solution was removed and 100 μL DMSO was added to dissolve the formazan crystals. Finally, the absorbance was measured at 570 nm using a Microplate Absorbance Reader (Biorad iMARK™, USA) and the cell viability was calculated.

2.6. Elemental fluorescence mapping

The cells were grown on sterile Malay film. After incubated with TiO_2 nanoparticles or TiO_2/DOX nanocomposite for 2 h, the cells were washed with PBS for 3 times and were fixed with 4% formaldehyde solution for 30 min and then washed with ultrapure water. Element fluorescence maps of cells were conducted at hard X-rays BL15U beamline at Shanghai Synchrotron Radiation Facility (Shanghai, China). Energy of X-ray was 10 keV, and beam spot was 0.5 × 0.5 μm. Scan time was 1 second at each step. Elemental maps of S, Cl, Ca, Ti, Fe, Cu and Zn in cells were acquired as described previously.[19]

2.7. Confocal laser scanning microscopy

The MCF-7 or MCF-7/ADM cells (1×10^5) were seeded into 35 mm culture dishes and incubated for 24 h. The growth media were then replaced by fresh DMEM, TiO_2/DOX nanocomposite or DOX alone containing DMEM at equivalent DOX concentration (5 μg mL^{-1}). After incubation for 2 h, cells were washed three times by PBS. Cells were fixed with 4% formaldehyde for 30 min, rinsed with PBS and then they were incubated with 0.2% Triton X-100 for 10 minutes, followed by washing with PBS. After the addition of 1% BSA solution to block the nonspecific binding sites, the cells were then stained with 50 μg mL^{-1} FITC–phalloidine for 1 h at room temperature and washed with PBS. Finally, the cells were stained with Hoechst 33342 (2 μg mL^{-1}) for 15 minutes, followed by washing with PBS. These culture dishes were examined with a Leica TCS SP5 confocal microscope (Leica Microsystems, Germany). Excitation and emission wavelengths (nm) used for Hoechst 33342, FITC–phalloidine and DOX were respectively 405 and 420 nm, 488 and 525 nm, 488 and 585 nm.

2.8. *In vitro* reversal of drug resistance for cancer cells

The MCF-7 or MCF-7/ADM cells were seeded into 96-well plates with a number of 1×10^4 cells per well. After incubation for 24 h, the culture media were replaced by fresh DMEM, TiO_2/DOX nanocomposite or DOX alone containing DMEM. The DOX concentrations were 1, 5, and 10 μg mL^{-1} corresponding to TiO_2/DOX nanocomposite or DOX alone containing DMEM. Subsequent experiments were performed as described above.

2.9. Statistical analysis

Data are presented as the mean ± standard deviation. The Student's t test was used for significance testing and $p < 0.05$ was considered to be statistically significant.

3. Results and discussion

3.1. Characterizations of TiO_2/DOX

The maximum loading efficiency of DOX onto TiO_2 surface was determined to be 1.1% with one mol of TiO_2 carrying 0.011 mol of DOX. However, in order to keep the stability of the TiO_2/DOX nanocomposite, the molar ratio of DOX to TiO_2 was adjusted to 0.55%. (For details see Fig. S4 of ESI.†)

As shown in Fig. 1A, UV-visible absorbance of TiO_2 showed a red shift after DOX loading, which suggested that the surface of TiO_2 was modified by ligand (DOX).[20] Since the loading amount of DOX was only 0.55%, its UV absorption was very weak compared to those of TiO_2 nanoparticles and TiO_2/DOX nanocomposite as shown in Fig. 1A.

The IR spectra of TiO_2, TiO_2/DOX and DOX are shown in Fig. 1B and the DOX molecular structure is presented in Fig. 1C. The IR spectrum (4000–900 cm^{-1}) of TiO_2 consisted of two absorption bands: (1) a broad band centered at 3428 cm^{-1} was

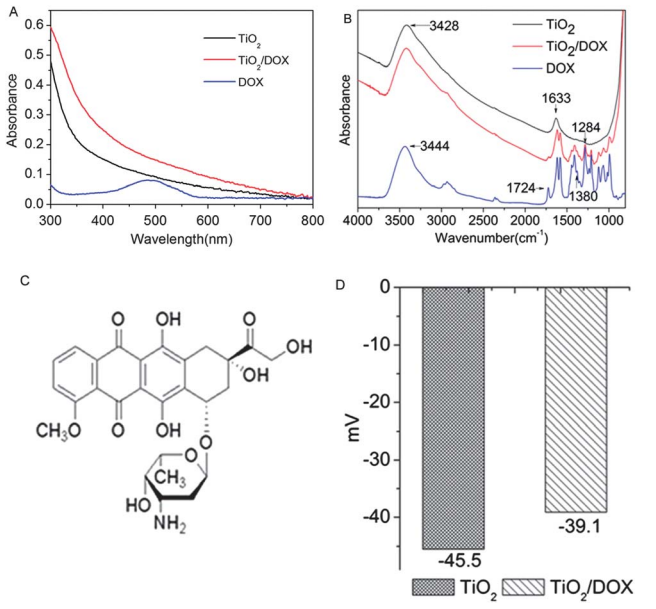

Fig. 1 (A) UV-visible absorption of TiO_2 nanoparticles, TiO_2/DOX nanocomposite and DOX solution. The absorption of TiO_2/DOX showed a red shift compared with TiO_2. (B) IR spectra of KBr pellets of TiO_2, TiO_2/DOX and DOX powder. The TiO_2/DOX corresponds to the main peaks of TiO_2 or DOX, but no new band was formed. (C) The molecular structure of DOX. (D) Zeta potential of TiO_2 nanoparticles and TiO_2/DOX nanocomposite. At pH 7.4, zeta potential of TiO_2 was −45.5 mV, and that of TiO_2/DOX was −39.1 mV.

due to a stretching mode of vibration of O–H groups linked to a TiO_2 surface, and (2) a narrower band at 1633 cm^{-1} was the scissoring vibration of adsorbed water molecules.[20] On the other hand, the IR spectrum of DOX contained many peaks of absorption. While a previous study proposed oxhydryl or carbonyl groups as binding functionalities to TiO_2 nanoparticles, it is possible that the binding peaks of DOX could be a broad band centered at 3444 cm^{-1} due to O–H stretching vibrations, a narrow band at 1724 cm^{-1} corresponding to stretching vibration of C=O group, a weak band at 1380 cm^{-1} could be associated with the vibration of O–H in phenolic hydroxyl moiety, and another narrow band at 1284 cm^{-1} is presumably due to vibration of O–H in alcoholic hydroxyl group.[16,21] Nonetheless, the absorption peaks for TiO_2/DOX are mainly the peaks of TiO_2 or DOX, but no new bands were observed. The results unambiguously confirmed that the DOX loading onto TiO_2 surface is indeed through a non-covalent bond process. Previous reports showed that the more likely TiO_2 binding sites of DOX were deduced to be the –OH, and the binding was labile.[12]

Moreover, the successful loading of DOX to the surface of TiO_2 was evident by the difference in zeta potential (Fig. 1D). At pH = 7.4, zeta potential of TiO_2 was −45.5 mV due to the surface hydroxyl groups. At the same pH value, after DOX was loaded onto TiO_2 surface, zeta potential of the resulting nanocomposite was found to be −39.1 mV due to amino group of DOX molecule indicating the adsorption of DOX onto TiO_2 surface was also *via* electrostatic interaction.

3.2. Size distribution and pH controlled drug release of TiO_2/DOX

The size distributions of TiO_2 and TiO_2/DOX are shown in Fig. 2A. The average diameter of TiO_2 was about 106 nm, and TiO_2/DOX was about 113 nm. The photographic images of TiO_2, TiO_2/DOX and DOX solutions are shown in Fig. 2A.

As shown in Fig. 2B, the size of TiO_2/DOX was changed from about 113 nm to 115 nm in seven days. It could be found that the size of TiO_2/DOX was changed very slowly, which indicated the TiO_2/DOX was stable in ultrapure water.

Furthermore, the pH sensitivity of DOX release was determined. Fig. 2C showed drug release kinetics of TiO_2/DOX at pH 7.4, 5.0 and 3.0 in buffer solution, which imitated the pH of physiological blood, endosome or lysosome, respectively. The similar acidity value for pH controlled drug release has been reported previously.[22] It could be observed that the cumulative release ratio of DOX was enhanced from 28% to 68% with the pH value decreased from 7.4 to 3.0 in 48 h. Protonation of DOX occurred at lower pH, that could release chemisorbed drug into the dialysis solution.[23] Moreover, the negative charge on TiO_2 surface could be turned into positive at acidic pH, which attenuated the electrostatic interaction between TiO_2 and DOX to enhance the drug release. The results indicated TiO_2/DOX was partially pH controlled drug release system.

3.3. Cytotoxicity of TiO_2 on human breast cancer cells

Although it has been demonstrated that TiO_2 nanomaterial is environmentally friendly and relatively nontoxic,[24] the drug-loading of TiO_2 was diluted to half of the maximum loading in this study, thereby enhancing the amount of TiO_2 in subsequent administration of the nanocomposite. Thus, *in vitro* cytotoxicity of high quantity of TiO_2 was determined by MTT (3-(4,5-dimethylthiazol-2-yl)-2,5-diphenyltetrazolium bromide) (Fig. 3). It could be estimated that up to 200 μg mL^{-1}, the TiO_2 does not exhibit any significant viability loss in both MCF-7 and MCF-7/ADM cells. A 200 μg mL^{-1} quantity of TiO_2 was used as the maximum dose in subsequent experiments.

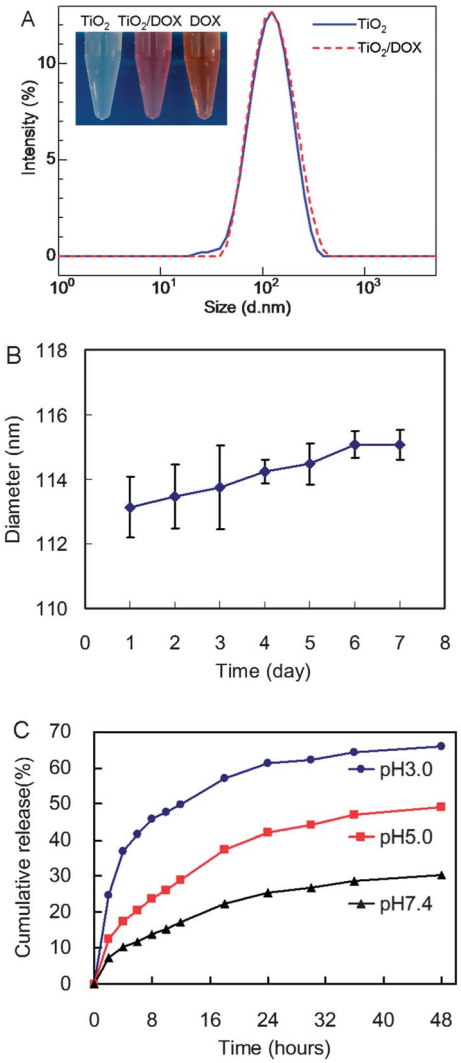

Fig. 2 (A) Size distribution of TiO_2 and TiO_2/DOX. Average sizes of TiO_2 or TiO_2/DOX were 106 and 112 nm respective. (B) Stability of TiO_2/DOX in ultrapure water. (C) Drug release of TiO_2/DOX at different pH value.

3.4. X-ray fluorescence maps of cancer cells

To acquire direct visual distribution of titanium arising from TiO_2 or TiO_2/DOX in cancer cells, the X-ray fluorescence microscope (XFM) was used to map elemental fluorescence of cancer cells. A hard X-ray beam of 10 keV energy was used at Shanghai Synchrotron Radiation Facility to excite elemental S, Cl, Ca, Ti, Fe, Cu and Zn in cancer cells, which have X-ray emission lines in 10 keV.[25] The biogenic element sulfur (blue)

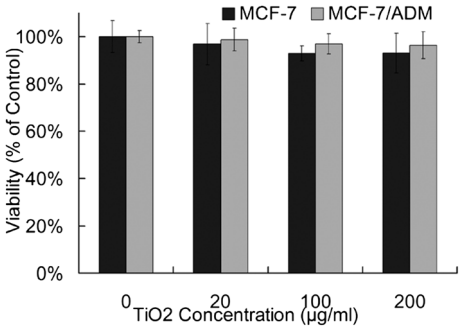

Fig. 3 Cytotoxicity of TiO_2 in human breast cancer MCF-7 and MCF-7/ADM cells with incubation time of 24 h. Data were expressed as the mean ± standard deviation of three experiments. Statistically significant differences were evaluated using the Student's *t* test.

was used to sketch cells as shown in Fig. 4. Element titanium was depicted as red or yellow (red and yellow respectively indicated low and high quantity of Ti). After incubation with 200 μg mL^{-1} TiO_2 or TiO_2/DOX for 2 hours, as shown in S and Ti overlapped pictures, most of Ti was distributed around the edge of cells. The XFM revealed that the Ti was mainly distributed in cytoplasm in both MCF-7 (Fig. 4A) and MCF-7/ADM (Fig. 4B) cells and not in their nuclei. It has already been demonstrated that TiO_2 nanoparticles are internalized by cancer cells *via* endocytosis to form endosomes having acidic environment around pH = 4 and that while DOX is loaded onto TiO_2 nanoparticles through a non-covalent interactions, it can also be released from the surface of TiO_2 in acidic environment.[26] Unfortunately, DOX could not be detected by XFM.

3.5. Intracellular localization of drugs

In order to investigate the behavior of intracellular DOX alone or TiO_2/DOX nanocomposite, the localization of the drug in MCF-7 or MCF-7/ADM cells was observed by confocal microscopy. Amount of DOX was adjusted to the same value (5 μg mL^{-1}) in the treatment of DOX alone or TiO_2/DOX nanocomposite. The FITC–phalloidine and Hoechst 33342 were used to label cell membrane (green fluorescence) and nucleus (blue fluorescence), respectively. As shown in Fig. 5A, the DOX alone treated MCF-7 cells showed red fluorescence and all of the DOX were located in the nucleus. This is in agreement with the widely accepted mechanism of cytotoxicity of DOX in which the cytotoxicity arises mainly from the direct intercalation of DOX into DNA and, subsequently, inhibition of DNA replication in nucleus.[13] In the treatment involving in TiO_2/DOX nanocomposite, most of the drugs were distributed in the nucleus, while some in granular form were located in the cytoplasm. Since DOX is a water-soluble species and will not aggregate to form granules, the granules can be the only of the TiO_2/DOX nanocomposite that can be invaginated by cells to form endosomes, but the drugs were not released completely as seen in the X-ray fluorescence microscopy (XFM). Fig. 5B shows intracellular localization of drugs in MCF-7/ADM cells. The cells treated by DOX alone showed a weak red fluorescence signal in the nucleus. Since multidrug resistance of cancer is

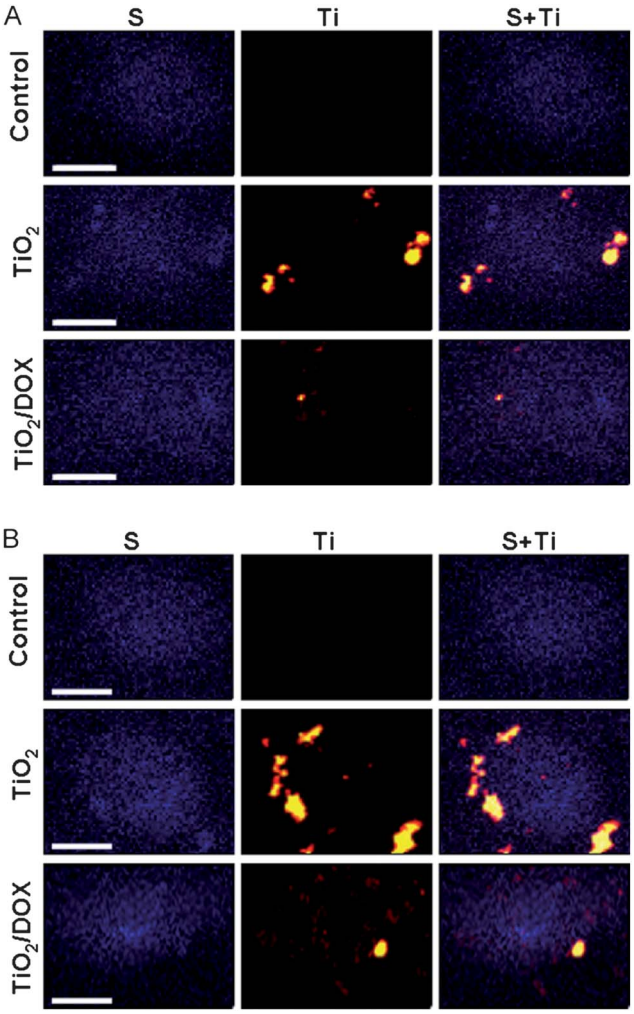

Fig. 4 X-ray fluorescence maps of (A) MCF-7 cells and (B) MCF-7/ADM cells treated with TiO_2 or TiO_2/DOX. Cells were incubated with TiO_2 or TiO_2/DOX at equivalent TiO_2 concentration (100 μg mL^{-1}) for 2 h. Scanning was performed using 10 keV incident energy with the scale bar as 20 μm. Beam spot was 0.5 × 0.5 μm and scan time was 1 second at each step. Blue fluorescence showed biogenic elemental sulfur in cells. Titanium of TiO_2 or TiO_2/DOX was showed as red or yellow (red and yellow, respectively, indicated low and high quantity of Ti).

associated with high expression of P-gp that can transport DOX,[27] the MCF-7/ADM cells can actively pump out free DOX leading to reduced nuclear drug accumulation. In comparison with DOX alone treatment, more red fluorescence was accumulated in cellular nuclear region with some red granules in cytoplasm of MCF-7/ADM cells in the case of combined TiO_2/DOX treatment. The red granules were found to be none other than TiO_2/DOX encapsulated endosomes that is in accordance with our presumption. Therefore, the DOX delivery to the cancer cells through TiO_2 nanocarriers should be *via* endocytosis in which the invaginated plasma membrane envelopes the TiO_2/DOX nanocomposite to form endosomes that can bypass the P-gp mediated drug pumping system for drug delivery.[28] The acidic environment of the endosomes should release DOX from TiO_2 surface and the released drugs could then interact with the DNA in the nuclei as an effective

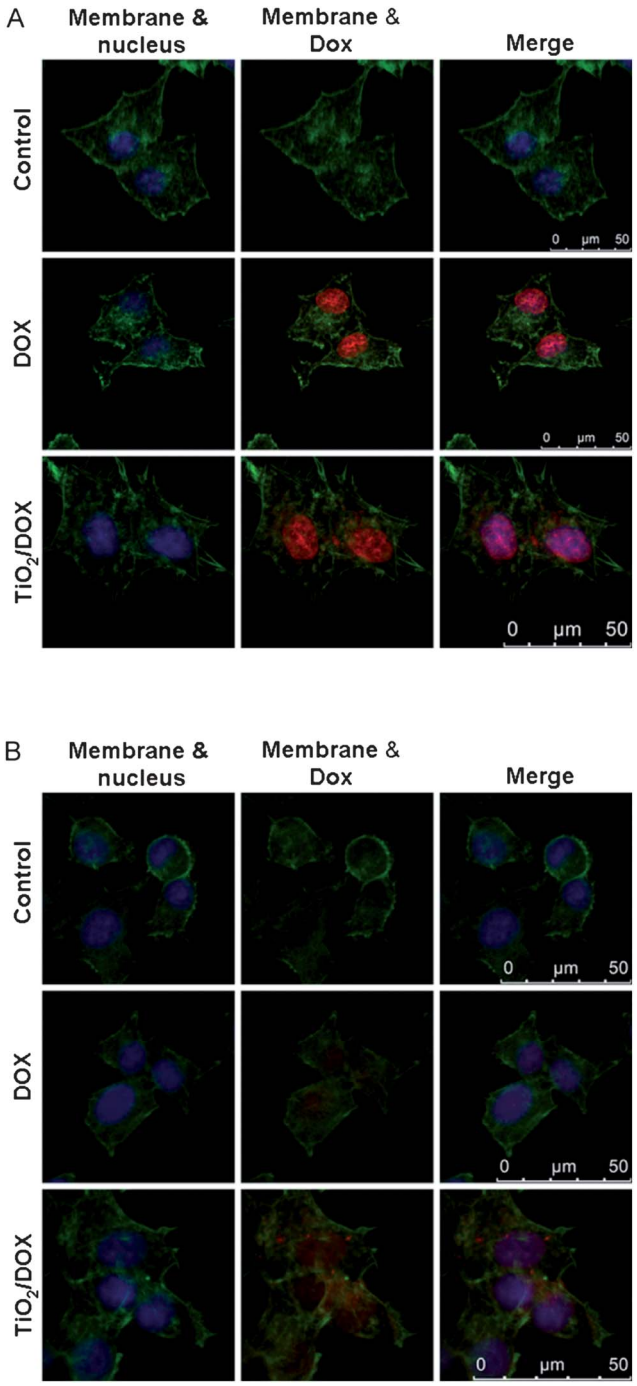

Fig. 5 Confocal microscopy images of cancer cells treated with DOX or TiO_2/DOX with the scale bar as 50 μm. (A) MCF-7 cells and (B) MCF-7/ADM cells, incubated with DOX or TiO_2/DOX at equivalent DOX concentration (5 μg mL^{-1}) for 2 h. Blue fluorescence showed Hoechst 33342 labeled nuclei, green fluorescence indicated FITC–phalloidine stained cell membrane, and red fluorescence was localization of DOX.

chemotherapeutic agent. Thus, more strong red fluorescence signals are evident in the nucleus, while some red granules are found in the cytoplasm. Nonetheless, the results do indicate that the TiO_2/DOX nanocomposites were part of pH controlled intracellular drug delivery system.

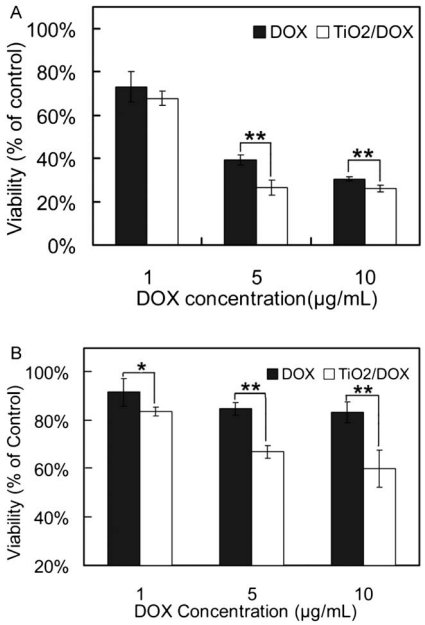

Fig. 6 Anticancer effects of DOX or TiO_2/DOX in human breast cancer cells. (A) MCF-7 cells and (B) MCF-7/ADM cells, incubated with DOX or TiO_2/DOX for 24 h. Data were expressed as the mean ± standard deviation of three experiments. Statistically significant differences were evaluated using the Student's *t* test (*$p < 0.05$; **$p < 0.01$).

3.6. Anticancer effects of DOX or TiO_2/DOX on cancer cells

Although enhanced accumulation of DOX in the nucleus was observed in TiO_2/DOX treated MCF-7/ADM cells, it is still unknown whether this enhanced drug accumulation could overcome the drug resistance of the cells and thus warrants further investigation through subsequent experiments. Fig. 6 shows anticancer effects of DOX alone and TiO_2/DOX nanocomposite in human breast cancer cells. Accordingly, for drug sensitive MCF-7 cells (Fig. 6A), TiO_2/DOX exhibited a slightly higher anticancer effect than that of DOX alone after 24 h incubation. In drug resistant MCF-7/ADM cells (Fig. 6B), DOX alone did not exhibit significant cytotoxicity, in fact only 16% of the cancer cells were killed even when DOX concentration was 10 μg mL^{-1}. However, the TiO_2/DOX nanocomposite transports the drug directly into cells *via* internalization forming endosomes that can bypass the P-gp mediated drug pumping system. Furthermore, the drug could be released easily in the acidic environment of endosomes or lysosomes, in which the pH was 4–5. Therefore, 40% of MCF-7/ADM cells were killed after they were treated with TiO_2/DOX nanocomposite containing 10 μg mL^{-1} of DOX indicating the enhanced anticancer effect of DOX by about 2.4 times in drug-resistant cells when compared to DOX alone. Evidently, TiO_2, as a pH triggered drug release system, can overcome the multidrug resistance in MCF-7/ADM cells, and thus enhances the anticancer activity of DOX.

4. Conclusions

In this work, DOX was loaded onto TiO_2 nanoparticles to form TiO_2/DOX nanocomposite. The nature of the interaction

between DOX and TiO_2 nanoparticles was determined by UV-visible spectra, IR spectra and zeta potentials. The results unambiguously confirmed that DOX is adsorbed onto TiO_2 nanoparticles *via* electrostatic interaction. In order to ensure greater stabilization of TiO_2/DOX nanocomposites, only half of the nanoparticle surface binding sites were utilized to load the drug. Since TiO_2/DOX nanocomposite is pH sensitive drug delivery system, DOX can be released from the surface of TiO_2 nanoparticles in the acidic environment of endosomes or lysosomes ~pH = 4–5 as indicated by drug release kinetics, X-ray fluorescence microscopy (XFM) and confocal microscopy. These results are different from those observed in our previous study.[12] The anticancer activity of TiO_2/DOX nanocomposite was evaluated in multidrug resistant MCF-7/ADM cells indicating 2.4 times anticancer activity of TiO_2/DOX nanocomposite with increase in accumulation of doxorubicin in MCF-7/ADM cells when compared with that of DOX alone. The mechanism of reversed multidrug resistance could be due to direct transfer of the drug through TiO_2/DOX nanocarrier into intracellular cytoplasm *via* internalization and then bypassing the P-gp mediated pumping system to release DOX (Scheme 2). Nonetheless, our study further demonstrates that TiO_2/DOX nanocomposite is part of pH-controllable and very promising drug delivery system to overcome the multidrug resistance in cancer chemotherapy.

Acknowledgements

This work was supported by Natural Science Foundation of China (Grant No. 51102251, 31128007, 51203175 and 31170964), the aided program for Science and Technology Innovative Research Team of Ningbo Municipality (Grant No. 2009B21005), and Hundred Talents Program (Grant No. 2010-735), CAS. The authors also thank Dr Keqiang Li from Ningbo No.2 Hospital for donating in, MCF-7 and MCF-7/ADM cells. Shanghai Synchrotron Radiation Facility at line BL15U (No. 12sr0012) used for X-ray fluorescent imaging is acknowledged. N.S.H. thanks the Chinese Academy of Sciences for the Visiting Professorship for Senior International Scientists (Grant No. 2011T2G19) and Northern Illinois University for granting the leave of absence.

References

1 G. Szakács, J. K. Paterson, J. A. Ludwig, C. Booth-Genthe and M. M. Gottesman, *Nat. Rev. Drug Discovery*, 2006, **5**, 219–234.
2 R. Singh and J. W. Lillard Jr, *Exp. Mol. Pathol.*, 2009, **86**, 215–223.
3 M. M. Gottesman and I. Pastan, *Annu. Rev. Biochem.*, 1993, **62**, 385–427.
4 D. Peer, J. M. Karp, S. Hong, O. C. Farokhza, R. Margalit and R. Langer, *Nat. Nanotechnol.*, 2007, **2**, 751–760.
5 L. S. Jabr-Milane, L. E. Vlerken, S. Yadav and M. M. Amiji, *Cancer Treat. Rev.*, 2008, **34**, 592–602.
6 K. Cho, X. Wang, S. Nie, Z. Chen and D. M. Shin, *Clin. Cancer Res.*, 2008, **14**, 1310–1316.
7 E. S. Lee, Z. Gao and Y. H. Bae, *J. Controlled Release*, 2008, **132**, 164–170.
8 S. Bhattacharyya, R. A. Kudgus, R. Bhattacharya and P. Mukherjee, *Pharm. Res.*, 2011, **28**, 237–259.
9 F. M. Kievit, F. Y. Wang, C. Fang, H. Mok, K. Wang, J. R. Silber, R. G. Ellenbogen and M. Zhang, *J. Controlled Release*, 2011, **152**, 76–83.
10 H. Meng, M. Liong, T. Xia, Z. Li, Z. Ji, J. I. Zink and E. N. Andre, *ACS Nano*, 2010, **4**, 4539–4550.
11 J. Wu, Y. Wang, X. Yang, Y. Liu, J. Yang, R. Yang and N. Zhang, *Nanotechnology*, 2012, **23**, 355101.
12 H. C. Arora, M. P. Jensen, Y. Yuan, A. G. Wu, S. Vogt, T. Paunesku and G. E. Woloschak, *Cancer Res.*, 2012, **72**, 769–778.
13 S. Yamaguchi, *Photochem. Photobiol.*, 2010, **86**, 964–971.
14 T. Paunesku, T. Ke, R. Dharmakumar, N. Mascheri, A. G. Wu, B. Lai, S. Vogt, J. Maser, M. Aslam, V. Dravid, R. Bergan and G. E. Woloschak, *Nanomed. Nanotechnol.*, 2008, **4**, 201–207.
15 L. Y. Zeng, W. Z. Ren, L. C. Xiang, J. J. Zheng, B. Chen and A. G. Wu, *Nanoscale*, 2013, **5**, 2107–2113.
16 Y. Chen, Y. Wan, Y. Wang, H. Zhang and Z. Jiao, *Int. J. Nanomed.*, 2011, **6**, 2321–2326.
17 Y. Qin, L. Sun, X. Li, Q. Cao, H. Wang, X. Tang and L. Ye, *J. Mater. Chem.*, 2011, **21**, 18003–18010.
18 A. G. Wu, T. Paunesku, E. M. Brown, A. Babbo, C. Cruz, M. Aslam, V. Dravid and G. E. Woloschak, *NANO*, 2008, **3**, 27–36.
19 T. Paunesku, T. Rajh, G. Wiederrecht, J. Maser, S. Vogt, N. Stojićević, M. Protic, B. Lai, J. Oryhon, M. Thuranuer and G. Woloschak, *Nat. Mater.*, 2003, **2**, 343–346.
20 T. Rajh, L. X. Chen, K. Lukas, T. Liu, M. C. Thurnauer and D. M. Tiede, *J. Phys. Chem. B*, 2002, **106**, 10543–10552.
21 G. Das, A. Nicastrl, M. L. Coluccio, F. Gentile, P. Candeloro, G. Cojoc, C. Liberale, F. De Angelis and E. Di Fabrizio, *Microsc. Res. Tech.*, 2010, **73**, 991–995.
22 F. Zhang, G. B. Braun, A. Pallaoro, Y. Zhang, Y. Shi, D. Cui, M. Moskovits, D. Zhao and G. D. Stucky, *Nano Lett.*, 2012, **12**, 61–67.
23 H. Zhang, C. Wang, B. Chen and X. Wang, *Int. J. Nanomed.*, 2012, **7**, 235–242.
24 M. Song, R. Zhang, Y. Dai, F. Gao, H. Chi, G. Lv, B. Chen and X. Wang, *Biomaterials*, 2006, **27**, 4230–4238.
25 E. A. Rozhkova, I. Ulasov, B. Lai, N. M. Dimitrijevic, M. S. Lesniak and T. Rajh, *Nano Lett.*, 2009, **9**, 3337–3342.
26 K. T. Thurn, H. Arora, T. Paunesku, A. Wu, E. M. Brown, C. Doty, J. Kremer and G. Woloschak, *Nanomed. Nanotechnol.*, 2011, **7**, 123–130.
27 M. D. Chavanpatil, Y. Patil and J. Panyam, *Int. J. Pharm.*, 2006, **320**, 150–156.
28 V. P. Torchilin, *AAPS J.*, 2007, **9**, E128–E147.